REYNOLDS DECOMPOSITION OF TURBULENCE CONTAINING SUPER-COHERENT STATES

R. J. Adrian, P. J. Sakievich, Y. T. Peet

Mechanical and Aerospace Engineering
School of Matter Transport and Energy,
Arizona State University
501 E. Tyler Mall, Tempe, AZ 85287
email: rjadrian@asu.edu

ABSTRACT

A vexing problem occurs in certain flows when long, but finite, time-average estimates of the mean flow fail to exhibit the symmetry properties imposed by boundary conditions and physics. The mean field becomes suspect, making it difficult, or even incorrect to apply Reynolds decomposition. The problem occurs when the flow exhibits "super-coherent" states, i.e. states of flow having coherence times much longer than the averaging times used in typical turbulence experiments. Turbulent Rayleigh-Bénard convection (RBC) is one such flow, and it will be used here as an example to illustrate and explain this phenomenon. The study focuses on a turbulent RBC experiment (Fernandes, 2001) in a 6.3:1 (diameter: depth) aspect-ratio vertical cylinder that supplemented time averaging with true ensemble averaging to achieve almost zero mean flow. To obtain a three-dimensional time-varying picture of the mechanisms at work, the experiment is simulated by direct numerical simulation of the Boussinesq equations (Sakievich *et al.*, 2016). Three types of super-coherent states, associated with the symmetries of the flow, are found to bias the mean flow, unless steps are taken to sample each state with equal probability.

INTRODUCTION

Reynolds decomposition is fundamental in the analysis of turbulence, and measurement of the mean flow must be accurate to within a small fraction of the turbulent fluctuation intensity to properly define the turbulent fluctuating field. The rules for averaging the results of turbulent flow experiments, physical or numerical, are quite simple: infinite averages over time are unbiased if the flow is statistically stationary and ergodic; infinite averages over space are unbiased if the flow is statistically homogeneous in the averaging direction(s) and ergodic; and finite averages converge to the infinite averages with small random error if they are performed over many thousand integral scales (in time or space). Lastly, convergence should be checked by repeated experiments.

These rules suffice in most situations, if the averaging domains are large enough to achieve converged statistics, but not always. In certain flows they do not guarantee unbiased results because, even if convergence is suggested by smoothness of the average, it may be much slower than expected, leading to physically incorrect results. Very slow convergence occurs when coherent structures of the flow, usually those of large scale, persist over times much longer than scale analysis or the integral time scale would suggest. We call structures having this property "super-coherent". The failure of the integral time scale to disclose super-coherence lays in the fact that it is composed of the time scales of motions of all sizes, such that the small-scale, short-time motions skew the correlation function to small times, thereby obscuring the long-time motions.

A more insidious problem with time averaging occurs when the flow locks into 'states' that do not possess all of the symmetry that the infinite time average must have. These seem to result from state-space bifurcations into basins of attraction that trap the dynamics for very long (or perhaps infinite), times only occasionally (or perhaps never) allowing natural transitions from one basin to another. In these cases, averages over long but finite times may sample only one of the states, or sample one state over a much longer time than another, creating a bias. It is necessary to either take much longer time averages, many times not an option, or to stimulate the transitions. The latter can be accomplished by stopping the experiment and starting a new one, so as to achieve identical, independent experiments, yielding a finite ensemble of equi-probable experiments. This approach holds true to the definition of an ensemble average, and so long as each state is realized with equal frequency, it is shown to improve convergence to the true infinite time average considerably (Fernandes, 2001).

Two new methods are introduced to reduce bias to one state or another in a finite time experiment. One involves sensing the times spent in the different states, and the other defines an efficient way to stop and restart the identical experiments so as to achieve independent realizations whose initial conditions occupy the various basins of attraction with the correct frequency of occurrence.

TURBULENT RAYLEIGH-BÉNARD CONVECTION

The ideal canonical form of RBC occurs in a horizontal layer of constant property fluid bounded by two infinitely wide horizontal plates, the warm bottom plate being heated uniformly and steadily, and the cool top plate being cooled in a similar manner to achieve either constant temperatures or constant mean heat flux. The unstable temperature stratification generates buoyancy forces within the fluid layer which then drive the flow. The Rayleigh number $Ra = \beta g \Delta T h^3 / \alpha \nu$, (where β is the coefficient of thermal expansion, g is the gravitational constant, ΔT is the temperature difference between the two heated plates, h is the plates' vertical separation, α is the thermal diffusivity and ν is the kinematic viscosity), is the primary dimensionless parameter and the Prandtl number $Pr = \nu / \alpha$ is often of less importance. A horizontal length scale (L) is also very important for determining the structure of the flow. The ratio of these two length scales is the aspect-ratio ($\Gamma = L/h$).

Linear instability of this system occurs at $Ra = 1708$, and it has the form of parallel, steady, two-dimensional roll-cells. With increasing Rayleigh number a sequence of more complicated finite amplitude laminar instabilities and transitions occurs (Busse & Whitehead, 1971, 1974; Busse, 1978), ending with steady, laminar hexagonal cells at about $Ra = 50,000$. Above $Ra = 10^5$ the flow becomes chaotic, and around $Ra = 10^6 - 10^7$ it is usually considered to be turbulent. Studies of the turbulent state (Chu & Goldstein, 1973; Garon & Goldstein, 1973; Willis & Deardorff, 1970; Fitzjarrald, 1976) were generally performed in square or rectangular test sections whose aspect ratios ranging from 1 to 80. Despite having fairly wide aspect-ratios, the experiments capable of sensing the flow velocity found non-zero mean flows, contrary to the zero-value

expected for infinite aspect-ratio. As noted above this puzzling result made application of Reynolds decomposition problematic. A similar phenomenon also appeared in unsteady non-penetrative convection, a very close relative of RBC in which the cool upper plate is replaced by an insulating plate (Adrian *et al.*, 1986). It could be hypothesized that side-walls and insufficient aspect-ratio might favor flow in one direction more than another. But the careful experiments of Krishnamurti & Howard (1981) in an annular test section also possessed mean flows around the annulus, despite the absence of side-walls, showing conclusively that non-zero mean flow in RBC derives from mechanics of the flow rather than experimental imperfections

LOW ASPECT-RATIO CONVECTION

Since the pioneering work of Castaing *et al.* (1989) on very high Rayleigh number turbulent convection in unit aspect-ratio cubes and cylinders that found the Nusselt number proportional to $Ra^{0.278}$ rather than the accepted value of $Ra^{1/3}$ most research has focused on very high Rayleigh numbers, necessitating low aspect-ratio test sections (see the review by Ahlers *et al.* (2009)) .

It is commonly observed that mean flow is prominent in unit aspect-ratio cubes and cylinders (Zocchi *et al.*, 1990; Bodenschatz *et al.*, 2000; Ahlers *et al.*, 2009)). Originally called the "wind of turbulence", the mean flow is part of a large-scale circulation that sweeps across the upper and lower plates, figure 1, creating a boundary layer that is of considerable interest regarding heat transfer.

Over the last two decades there has been a strong focus in the RBC community on understanding the scaling of the Nusselt number (Nu) with respect to Ra and Pr. As the years have progressed ever larger Ra have been reached in experimental and numerical studies with the goals of defining the scaling behavior and reaching the "ultimate" state for turbulent convection that was first proposed by Kraichnan (1962). Many different scaling laws for characterizing the heat transfer scaling in RBC systems have been proposed (Ahlers *et al.*, 2009) , but the most seminal and enduring work over the last 20 years is the theory proposed by Grossmann & Lohse (2000). Grossmann and Lohse's initial publication for a unifying theory to predict the scaling of the Reynolds number (Re) and Nusselt number (Nu) in turbulent RBC for any given Pr and Ra occurred in 2000 and has been improved by several additional publications (Grossmann & Lohse, 2001, 2002, 2003, 2004; Stevens *et al.*, 2013). This theory relies on three main assumptions for the flow field: statistical stationarity, a single dominant velocity scale represented by a mean wind, and characteristic boundary layer thicknesses for respective kinematic and thermal fields.

The majority of numerical and experimental studies have been performed in unit Γ boxes and cylinders. The "wind of turbulence" concept is often used to describe the flow structure in these small Γ domains. The "wind of turbulence" is characterized by a single roll-cell, or large-scale circulation (LSC), which spans the height and width of the cell, see figure 1. This roll-cell creates boundary layers along the side walls and thermally active top and bottom plates which are well described by the Prandtl-Blasius profiles according to Grossmann & Lohse (2000). While the theory has proven remarkably robust in predicting the scaling of Nu, the underlying assumptions are not guaranteed to hold at larger Γ where the large-scale structure of the flow departs from the concept of a single LSC.

For example, du Puits *et al.* (2007) clearly showed that the "wind of turbulence" breaks down as Γ increases by performing experiments in air over a wide range of $\Gamma = 1 - 11$ and $Ra = 10^8 - 10^{11}$. This has been further corroborated by numerical studies of Bailon-Cuba *et al.* (2010) ($Ra = 10^7 - 10^9$, $\Gamma = 0.5 - 11.0$) and Sakievich *et al.* (2016) ($Ra = 10^8$, $\Gamma = 6.3$) that reveal complex multi-dimensional patterns for roll-cells in moderate Γ con-
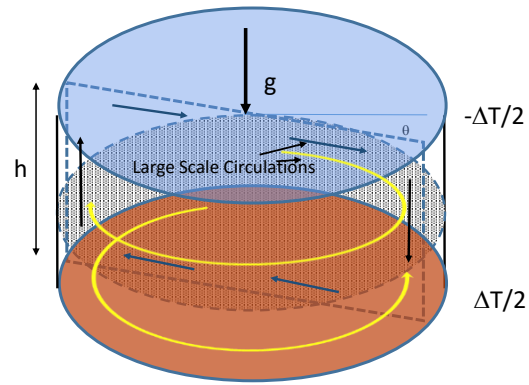

Figure 1. Conceptual diagram of the wind of turbulence in a $\Gamma = 1$ cell. The dotted plane illustrates the one of the infinite possibilities for the azimuthal orientation of the LSC. The yellow vectors indicate the directions for azimuthal drift.

tainers with sidewalls. In a recent conference Stevens *et al.* (2016) presented a numerical study that outlined the spatial extent needed to support fully developed superstructures in a periodic domain at $Ra = 10^8$ and $Pr = 1$. Stevens *et al.* (2016) found that $\Gamma \geq 32$ is required to support the full structure of the flow field, and that measured Nu departs from the Grossmann-Lohse theory at least in the region $1 \leq \Gamma \leq 4$. These variations from the standard picture of $\Gamma = 1$ RBC show that the physics of thermal convection is not fully described by the unit Γ case, and that there is a clear value in returning to large Γ studies that were prevalent several decades ago.

Very slowly evolving coherent motions have been observed in experimental studies and numerical simulations of wide aspect-ratio, turbulent Rayleigh-Bénard convection. The time scales on which they evolve make it extremely difficult to achieve statistically-converged results during the finite run times of numerical simulations. In this paper, we present a novel procedure of manipulating the turbulent flow states and performing statistical averaging in a way that mitigates these problems and yields the flow statistics that are close to the results of experiments which, in turn, approach the infinite-time average.

SUPER-COHERENCE AND STATES OF TURBULENT RBC IN AN ASPECT-RATIO 6.3:1 CYLINDER

FERNANDES EXPERIMENT

At first blush one is tempted to attribute LSCs to low aspect ratio, but as mentioned earlier, mean flow patterns have been observed in wider aspect-ratios, as well. The experiment by Fernandes (2001) employed a $914mm \times 914mm$ rectangular convection cell with an interior cylindrical domain of diameter $760mm$ and height $120mm$ defined within a thin, circular acetate wall. The aspect ratio for the cylinder was 6.3:1. With the intent of making the side-wall of the cylinder more passive thermally, convection occurred outside the cylinder as well as inside.

PRESENT SIMULATION

In our recent work we studied the large-scale structures in a 6.3 Γ cylindrical RBC cell via direct numerical simulation (DNS) (Sakievich *et al.*, 2016). This simulation was setup to mirror an experiment conducted by Fernandes (2001). After smoothing out the small-scales with a running time average we observed that the flow organized itself into a hub and spoke like pattern with an updraft in
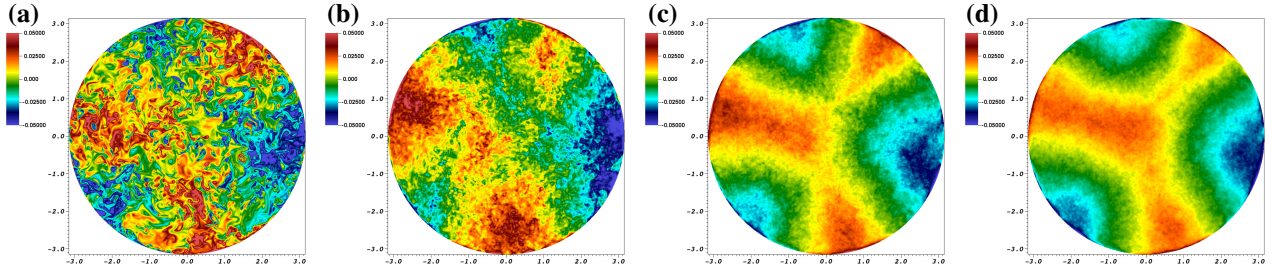
Figure 2.   Temperature at the mid-plane of the cell plotted with different temporal filtering timescales: instantaneous (a), 1 eddy turnover (b), 10 eddy turnovers (c), 20 eddy turnovers (d).
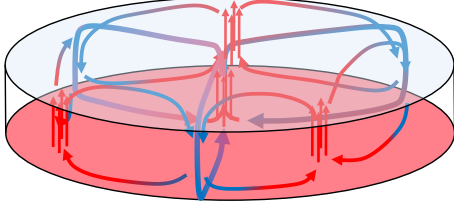

Figure 3.   Possible patterns at $\Gamma = 6.3$. This pattern is characterized by large-scale updraft in the center, and six large-scale drafts of alternating direction along the cell's side walls. Three dimensional roll-cells are created by connecting each updraft with the neighboring downdrafts.
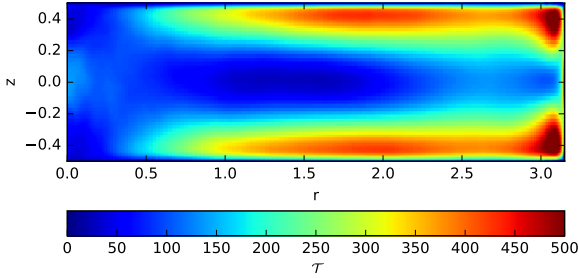

Figure 4.   Integral timescale for the 6.3 Γ simulation with seperation times expressed in freefall time units ($t_f = \sqrt{H/\beta g \Delta T}$)

the central region of the cell, and 6 alternating up- and down-drafts near the outer wall. The hub in this pattern is the central thermal and the spokes are the vortex lines that form between drafts of opposing direction along the outer wall. A conceptual illustration of the observed pattern's thermal signature is provided in figure 3. Very similar patterns were seen in the numerical study by Bailon-Cuba *et al.* (2010). The large-scale patterns in Sakievich *et al.* (2016) and Bailon-Cuba *et al.* (2010) showed no azimuthal drift or vertical reversal over at least 600 free fall time units ($t_f = \sqrt{h/\beta g \Delta T}$) in numerical simulations. From this we can infer that the large-scale patterns in turbulent RBC are remarkably stable at large Γ.

We will refer to the observed pattern in figure 3 as $state^+$ because the central column of fluid is an updraft. The persistence of the central column destroys the statistical homogeneity at the center of the cell over the set of realizations in $state^+$. This stands in direct conflict with the idea that as Γ is increased the central region of the cell should approach the infinite Γ case which is statistically homogeneous over horizontal planes. Clearly, additional states must exist in the infinite ensemble of realizations for this flow, and these

states are not represented in this data set even though it was sampled over more than $600 t_f$. If the temporal sampling were sufficiently extended to truly approach the infinite-time average then an event must occur that will drive the flow into other states. Possible states should, at the very least, include rotations about the central axis, and a reorganization of the large-scales to where the central region of the cell is characterized by a downdraft. We will refer to downdraft organization as $state^-$.

States that are simply a shift in the pattern's orientation can easily be accounted for by averaging in the homogenous azimuthal direction, as would be sufficient in a low Γ case. However, the downdraft pattern in large Γ case will require another state of the flow to be sampled. Without this additional state the data set can be considered a conditional average of the infinite time field based on the updraft large-scale organization. The realizations of the flow in this data set can not be truly statistically independent because the large-scale structures remain highly correlated throughout the time scales achievable in the simulations.

In this paper, we propose a simple modification of the conventional sampling and averaging procedures that allows us to select initial conditions for the effective ensemble averaging in a controlled way. With this technique, the additional states that will be sampled are created to possess certain properties (for example, a central downdraft versus updraft) that are missing in the "base" realization. By deliberately constructing and sampling specifically manufactured conditions that sample all states, we ensure that the statistics converge to an unbiased estimate of the infinite-time average using a relatively small number of realizations. For example, in this paper we achieve significantly improved statistics with only two realizations, sampling over $state^+$ and $state^-$ as discussed below. This technique can be used to expand the statistical significance of numerical data sets and extend the number of *independent* realizations that can be studied. We will illustrate this technique using our RBC data set, but it can potentially be applied to other flows where there are symmetries that allow solutions in multiple states.

The main idea behind our technique is to transform an instantaneous realization from the numerical data set into an initial condition for a different "super-coherent" state that possesses a desired organization in a large-scale structure. For this, we explore symmetries in the inhomogeneous directions. In addition, we require that the transformed data set evolves according to the governing equations. Our central goal for the manipulation performed in this paper is to reverse the flow direction in a central column (updraft versus down-draft) corresponding to $state^+$, identified in figure 2, and its reflection, $state^-$. We recognize that other symmetries (for example, based on the direction of the azimuthal rotation) can also produce other turbulent states.

To reverse the flow direction in the central column, we recast the field so that the structures falling from the cool top plate appear as structures rising from the warm bottom plate and vice versa.
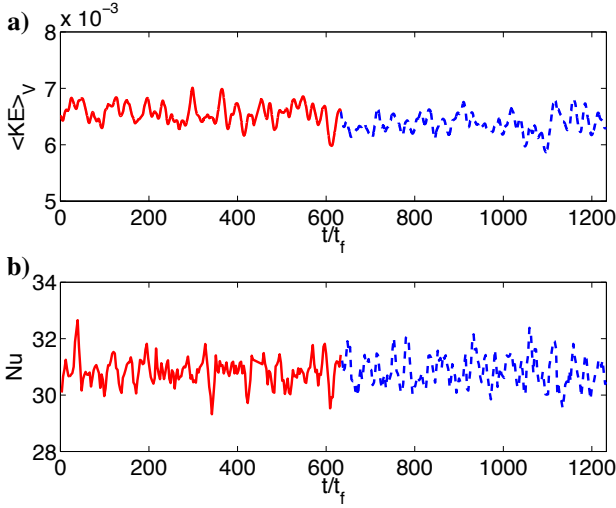
Figure 5. Temporal evolution of the volume average kinetic energy (a), and Nusselt number (b) are shown in the plots above. $state^-$ (- -, blue) was initialized from the last time step of $state^+$ (–, red).

Switching states is performed by transforming the vertical velocity component, vertical coordinate and temperature of a developed turbulent data set at every grid point in the simulation. The formulas for performing this switch are as follows:

$$(x^+, y^+, z^+) \rightarrow (x^-, y^-, z^-) : x^- = x^+, y^- = y^+, z^- = z_t + z_b - z^+, \quad (1)$$

$$w^-(x^-, y^-, z^-) = -w^+(x^+, y^+, z^+), \quad (2)$$

$$\theta^-(x^-, y^-, z^-) = \theta_t + \theta_b - \theta^+(x^+, y^+, z^+). \quad (3)$$

All other variables remain unchanged, for example, $u^-(x^-, y^-, z^-) = u^+(x^+, y^+, z^+)$ etc. Here, the subscripts t and b refer to the values at the top and bottom boundaries the superscripts + and − refer to the flow states, z, θ and w are the vertical coordinate, dimensionless temperature and vertical velocity, respectively. The transformation provided by equations (1)-(3) reflects all variables in the flow about the midplane and preserves the Navier-Stokes equations with the Boussinesq approximation, continuity equation and thermal energy equation exactly. The plots in figure 5 show identical signatures in the volume averaged kinetic energy and Nusselt number as the transition from $state^+$ to $state^-$ takes place. These results verify that this methodology preserves the continuity in volume average quantities, such as kinetic energy and total heat flux, during the state transition. Utilizing this technique to transition between converged states with long term statistical significance has the potential to improve statistical convergence in DNS studies of RBC at a significant reduction in computational expense.

To illustrate this point we have included a comparison with the statistical profiles from experiments of Fernandes (2001) and our previous work (Sakievich *et al.*, 2016) in figure 6. These profiles have been normalized by Deardorff's velocity scale $w* = (\beta g Q_o h)^{1/3}$ (Deardorff, 1970) where Q_o is the kinematic heat flux.

The profiles generated in figure 6 are taken from within the core region of the 6.3 Γ RBC cell with a radius of $0.925h$. It should be noted that the experimental mean vertical velocity profiles decrease in magnitude and the r.m.s vertical velocity profile's magnitude increases with Ra. Since the forcing within the cell increases with Ra the characteristic instantaneous velocity increases as the vertical r.m.s profile indicates. We hypothesize that the reason for the
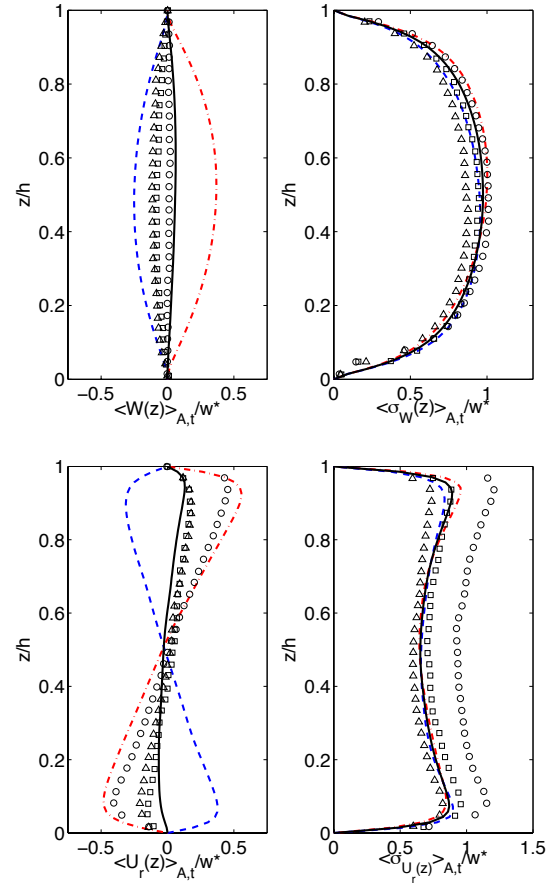

Figure 6. Ensemble and horizontally averaged mean (left) and r.m.s. (right) vertical (top) and radial (bottom) velocity profiles normalized by Deardorff's velocity scale $w*$: DNS: $Ra = 9.6 \times 10^7$, where red $(-\cdot)$ is $state^+$, blue (- -) is $state^-$ and black (–) is the average of $state^+$ and $state^-$; Experiment: $Ra = 6 \times 10^7$ (△), $Ra = 2 \times 10^8$ (□), $Ra = 1 \times 10^9$ (○)

decay of the mean velocity in the experimental profiles is that the antisymmetric states were more evenly accounted for in Fernandes ensemble averages with higher Ra (Fernandes, 2001). When the original DNS results ($state^+$ only) are compared against the experiment we see that the r.m.s profiles fall within ~ 11% in a pointwise comparison and that the mean profiles are dramatically over predicted. However, when the $state^+$ and $state^-$ are averaged together, the mean velocity profiles are very close to the expected (zero) value of the infinite-time average and the r.m.s profiles show an excellent match with the experimental results. This is truly remarkable when one considers that each instance of Fernades' ensemble average (with the total of 300 instances) was also temporally averaged over a greater time period than our entire simulation. By our estimates it would take us $O(10^8)$ CPU hours to recreate Fernandes experiment on our current grid (and the ability to recreate the desired uncorrelated large-scale patterns without targeted transformations as proposed here still could not be guaranteed). However, the results presented in this paper took $O(10^5)$ CPU hours to produce. Perhaps the most exciting observation is that the profiles in figure 6 clearly show that we were able to obtain a net downdraft in the central region of the cell over the sampling time of our second state. This shows that we were able to perform a targeted manipulation of instantaneous data to trigger a new state of the large-scale structures.

SUMMARY AND CONCLUSIONS

In summary we have discussed the challenges in obtaining the flow statistics that would converge to an infinite-time average in numerical simulations of turbulent flows and the bias that can be introduced due to insufficient sampling of flow states. Failure to recognize insufficient sampling can lead to variance in the statistics of stationary processes which are due to the correlation of slowly evolving large-scale structures that can persist well beyond the standard integral time scales. We used our recent numerical simulation of a 6.3 Γ RBC cell to provide an example of how this can occur. The results from this simulation were obtained with a high-order method and were numerically well resolved, as well as yielded longer than average temporal sampling Sakievich *et al.* (2016), but the central region of the cylinder showed inhomogeneous nature due to a large-scale updraft persisting in the cell's core. The only way to resolve this issue is to average these results with another state of the flow field with a downdraft in the center. We then presented a methodology for triggering this state using the inherent symmetries in the inhomogeneous vertical direction that didn't alter the net kinetic or thermal energy in the fully developed turbulent field. The application of this methodology showed that a net downdraft was indeed created in the region of interest and that this downdraft remained dominant over at least the same temporal averaging period that was used to collect the first flow state. This method has the potential for application to other flows that have multiple, long-lived states and an exploitable symmetry.

REFERENCES

Adrian, R. J., Ferreira, R. T. D. S. & Boberg, T. 1986 Turbulent thermal convection in wide horizontal fluid layers. *Experiments in Fluids* **4**, 121–141.

Ahlers, Guenter, Grossmann, Siegfried & Lohse, Detlef 2009 Heat transfer and large scale dynamics in turbulent rayleigh-bénard convection. *Reviews of modern physics* **81** (2), 503.

Bailon-Cuba, J., Emran, M. S. & Schumacher, J. 2010 Aspect ratio dependence of heat transfer and large-scale flow in turbulent convection. *Journal of Fluid Mechanics* **655**, 152–173.

Bodenschatz, Eberhard, Pesch, Werner & Ahlers, Guenter 2000 Recent developments in rayleigh-bénard convection. *Annual review of fluid mechanics* **32** (1), 709–778.

Busse, FH 1978 Non-linear properties of thermal convection. *Reports on Progress in Physics* **41** (12), 1929.

Busse, FH & Whitehead, JA 1974 Oscillatory and collective instabilities in large prandtl number convection. *Journal of Fluid Mechanics* **66** (01), 67–79.

Busse, F He & Whitehead, JA 1971 Instabilities of convection rolls in a high prandtl number fluid. *Journal of Fluid Mechanics* **47** (02), 305–320.

Carati, D., Wray, A. & Cabot, W. 1996 Ensemble averaged dynamic modeling. Center for Turbulent Research, Proceedings of the Summer Program.

Castaing, Bernard, Gunaratne, Gemunu, Heslot, François, Kadanoff, Leo, Libchaber, Albert, Thomae, Stefan, Wu, Xiao-Zhong, Zaleski, Stéphane & Zanetti, Gianluigi 1989 Scaling of hard thermal turbulence in rayleigh-bénard convection. *Journal of Fluid Mechanics* **204**, 1–30.

Chu, TY & Goldstein, RJ 1973 Turbulent convection in a horizontal layer of water. *Journal of Fluid Mechanics* **60** (01), 141–159.

Coleman, G. N., Kim, J. & Spalart, P. R. 2000 A numerical study of strained three-dimensional wallbounded turbulence. *Journal of Fluid Mechanics* **417**, 025112.

Deardorff, James W 1970 Convective velocity and temperature scales for the unstable planetary boundary layer and for rayleigh convection. *Journal of the Atmospheric Sciences* **27** (8), 1211–1213.

Fernandes, R. L. 2001 The spatial structure of turbulent rayleigh-benard convection. PhD thesis, University of Illinois, Urbana, IL.

Fernandes, R. L. & Adrian, R. J. 2002 Scaling of velocity and temperature fluctuations in turbulent thermal convection. *Exp. Thermal Fluid Science* **26**, 355–360.

Fitzjarrald, Daniel E 1976 An experimental study of turbulent convection in air. *Journal of Fluid Mechanics* **73** (04), 693–719.

Garon, AM & Goldstein, RJ 1973 Velocity and heat transfer measurements in thermal convection. *The Physics of Fluids* **16** (11), 1818–1825.

Grossmann, Siegfried & Lohse, Detlef 2000 Scaling in thermal convection: a unifying theory. *Journal of Fluid Mechanics* **407**, 27–56.

Grossmann, Siegfried & Lohse, Detlef 2001 Thermal convection for large prandtl numbers. *Physical Review Letters* **86** (15), 3316.

Grossmann, Siegfried & Lohse, Detlef 2002 Prandtl and rayleigh number dependence of the reynolds number in turbulent thermal convection. *Physical Review E* **66** (1), 016305.

Grossmann, Siegfried & Lohse, Detlef 2003 On geometry effects in rayleigh–bénard convection. *Journal of Fluid Mechanics* **486**, 105–114.

Grossmann, Siegfried & Lohse, Detlef 2004 Fluctuations in turbulent rayleigh–bénard convection: the role of plumes. *Physics of Fluids* **16** (12), 4462–4472.

Kraichnan, Robert H 1962 Turbulent thermal convection at arbitrary prandtl number. *The Physics of Fluids* **5** (11), 1374–1389.

Krishnamurti, Ruby & Howard, Louis N 1981 Large-scale flow generation in turbulent convection. *Proceedings of the National Academy of Sciences* **78** (4).

du Puits, Ronald, Resagk, Christian & Thess, André 2007 Breakdown of wind in turbulent thermal convection. *Physical Review E* **75** (1), 016302.

Sakievich, PJ, Peet, YT & Adrian, RJ 2016 Large-scale thermal motions of turbulent rayleigh–bénard convection in a wide aspect-ratio cylindrical domain. *International Journal of Heat and Fluid Flow* **61**, 183–196.

Stevens, Richard, Verzicco, Roberto & Lohse, Detlef 2016 Superstructures in rayleigh-benard convection. In *APS Meeting Abstracts*.

Stevens, Richard JAM, van der Poel, Erwin P, Grossmann, Siegfried & Lohse, Detlef 2013 The unifying theory of scaling in thermal convection: the updated prefactors. *Journal of fluid mechanics* **730**, 295–308.

Willis, GE & Deardorff, JW 1970 The oscillatory motions of rayleigh convection. *Journal of Fluid Mechanics* **44** (4), 661–672.

Zocchi, G., Moses, E. & Libchaber, A. 1990 Coherent structures in turbulent convection, an experimental study. *Physica A* **166**, 387–407.